# Symmetric bent-core mesogens with *m*-carborane and adamantane as the central units†‡

**Damian Pociecha,[a] Kiminori Ohta,[b] Adam Januszko,[c] Piotr Kaszynski*[c] and Yasuyuki Endo[b]**

***Received 20th December 2007, Accepted 11th March 2008***
***First published as an Advance Article on the web 8th April 2008***
**DOI: 10.1039/b719629f**

Several members of two homologous series of symmetric bent-shaped compounds with either *m*-carborane or adamantane (**1[*n*]** or **2[*n*]**, $n = 9$–13) in the central position were synthesized and investigated by optical, calorimetric, X-ray diffraction, and electro-optical methods. Results show that the two shortest members of the *m*-carborane series, **1[9]** and **1[10]**, exhibit an intercalated lamellar B6 phase. The adamantane derivatives **2[9]**–**2[13]** display a monotropic weakly birefringent soft crystalline or crystalline phase with homochiral domains. Neither phase undergoes polarization switching in an electric field.

## Introduction

Bent-core molecules, in which mesogenic units are attached to the central ring at an angle of about 120°, have been intensively investigated over the past decade.[1–3] Prompted by the discovery of electrooptical switching in one such achiral bent-core compound,[4] subsequent detailed investigations have uncovered spontaneous formation of homochiral domains, supramolecular chirality, and polar phases in many achiral bent-core mesogens. To date, several liquid crystalline phases (banana phases) have been identified in this new class of materials.[1,5]

As part of an effort to better understand structure–properties relationships in bent-core mesogens and to develop a rational design for molecules with desired polar properties, many series of compounds were prepared and investigated by diffraction, optical, and dielectric methods. Typically, planar central units such as 1,3-disubstituted benzene, 2,6-disubstituted pyridine, 2,7-disubstituted naphthalene, 3,4′-disubstituted biphenyl, and some 5-membered heteroaromatic rings have been used in the design of such bent-core molecular systems.[1,3] Occasionally, the central ring has an additional small substituent, which modifies the polar properties and packing of the molecules. The use of non-aromatic rings as the central unit is very rare. Examples include tetrahydropyran ring[6] and a recently reported pyrazabole,[7] which, in spite of its sterically demanding "roof" shape, supports the formation of nematic and soft crystalline banana phases.[7]

The use of large, bulky central groups in bent-core mesogens was avoided because of the belief that molecules with planar rings are necessary for achieving close packing in the fluid phase and the formation of banana phases. Also there are only a few possible candidates for such sterically demanding and conformationally rigid connectors. Among those are *m*-carborane and adamantane, which are approximately spherical and provide the desired connectivity patterns with an angle between the substituents of approximately 120°. The former is an inorganic boron cluster[8,9] with $C_{2v}$ point group symmetry and a moderate dipole moment of 2.85 D.[10] Adamantane, in contrast, is a non-polar, $T_d$-symmetric hydrocarbon.

Here we report the preparation and characterization of the first bent-shaped compounds in which *m*-carborane, in series **1[*n*]**, and adamantane, in series **2[*n*]**, serve as the bulky central connectors (Fig. 1).

## Results and discussion

### Synthesis

The two series of compounds were prepared by reaction of carboxylic acid **3[*n*]** with either 1,7-bis(4-hydroxyphenyl)-*m*-carborane (**4a**) or 1,3-bis(4-hydroxyphenyl)adamantane (**4b**) following a general procedure (Scheme 1).[11]

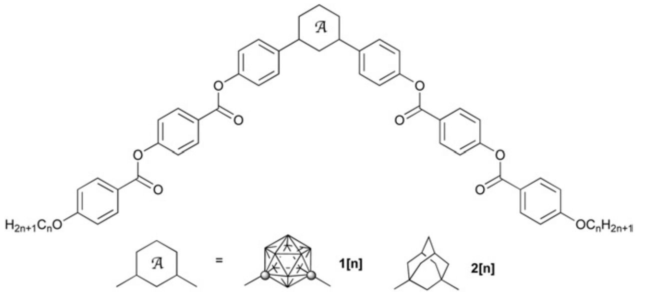

**Fig. 1** Two series of compounds derived from *m*-carborane (**1[*n*]**) and adamantane (**2[*n*]**). In *m*-carborane, each vertex represents a BH fragment and each sphere is a carbon atom.

---

[a] *Department of Chemistry, Warsaw University, Al. Zwirki i Wigury 101, 02-089 Warsaw, Poland*
[b] *Tohoku Pharmaceutical University, 4-4-1, Komatsushima, Aoba-ku, Sendai, 981-8558, Japan*
[c] *Organic Materials Research Group, Department of Chemistry, Vanderbilt University, Nashville, 37235, TN, USA. E-mail: piotr.kaszynski@vanderbilt.edu; Fax: +1-615-343-1234; Tel: +1-615-322-3458*

† This paper is part of a *Journal of Materials Chemistry* theme issue on Liquid Crystals Beyond Display Applications. Guest editor: Carsten Tschierske.

‡ Electronic supplementary information (ESI) available: Synthesis and analytical details for all compounds, transition temperatures for **3[*n*]** and **5[*n*]**, powder XRD for **2[11]** and electrooptical response for **1[9]**. See DOI: 10.1039/b719629f

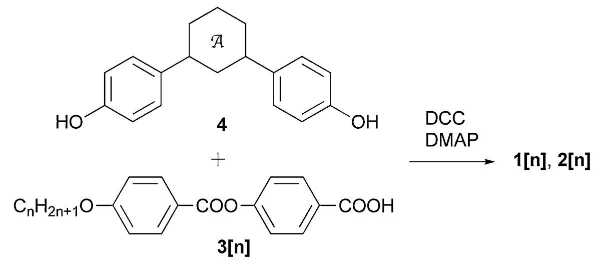

Scheme 1

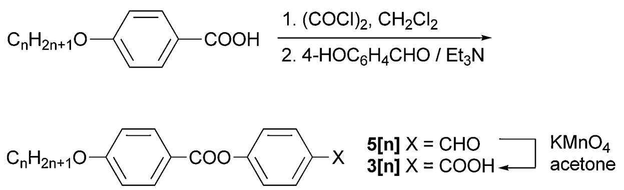

Scheme 2

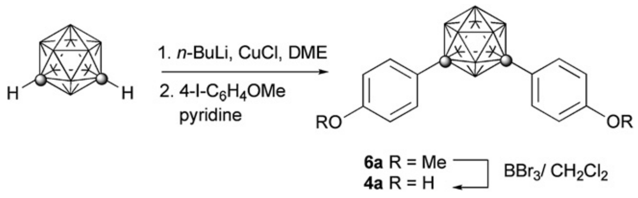

Scheme 3

Carboxylic acids[12] **3[*n*]** were prepared by oxidation of aldehydes **5[*n*]**, which were obtained according to a general literature procedure[13] (Scheme 2). The bisphenol **4a** was obtained by demethylation of dimethoxy derivative **6a** with $BBr_3$ (Scheme 3). Compound **6a** was prepared by arylation of *m*-carborane with 4-iodoanisole according to a general procedure.[14]

## Thermal analysis

Phase transition temperatures and enthalpies for series **1[*n*]** and **2[*n*]** are shown in Table 1. Phase structures were assigned on the basis of microscopic textures observed using a birefractive setup.

Analysis of the carborane series **1[*n*]** revealed that all melt about 155 °C and only the two lowest members of the series exhibit liquid crystalline behavior. The nonyloxy derivative **1[9]** exhibits an enantiotropic smectic phase, which easily supercools to about 130 °C before it crystallizes. In the next homolog, **1[10]**, the phase becomes monotropic and it appears 10 K below the melting point (Table 1). The clearing transitions for both compounds have the enthalpy change of nearly 18 kJ $mol^{-1}$.

The nonyloxy derivative **1[9]** exhibits a rich solid-state polymorphism. A virgin sample of **1[9]** shows two high-enthalpy Cr–Cr transitions at 99 °C and at 140 °C and a melting transition at 154 °C. In the second heating cycle, the low temperature Cr–Cr transition is absent and the melting transition appears at 148 °C. Higher homologues exhibit a low energy Cr–Cr transition at about 120 °C.

DSC analysis of the adamantane series **2[*n*]** did not reveal a mesophase formation. All compounds melt to an isotropic phase at about 180 °C and crystallize upon cooling with a small (0.5–5 K) hysteresis of the transition temperature. In addition, several broad Cr–Cr transitions are observed with the most common one at about 105 °C.

## Optical analysis

Microscopic observations of **1[9]** and **1[10]** confirmed the formation of a mesophase. Upon cooling between two glass slides both compounds form regular fan-shaped textures with additional thin lines and small areas of different birefringence (Fig. 2A). Removing the top cover glass by shearing and applying mechanical stress resulted in the formation of a schlieren texture as shown in Fig. 2B. No homeotropic region of the sample was observed in either of the textures. Considering the bent-core geometry of the molecules, such textures can be attributed to an intercalated lamellar B6 phase.[15,16]

Although DSC did not show mesophase formation in series **2[*n*]**, microscopic observations revealed that upon fast cooling from the isotropic phase all adamantane derivatives form a weakly birefringent phase with a dark non-characteristic texture. The texture exhibits optical activity (OA), and domains with opposite OA sign always coexist and have comparable areas (Fig. 3). The texture does not respond to electric field. However, cooling of the sample in the field leads to a texture with larger homochiral domains. At temperatures about 15 K below melting, the sample hardens and forms a glassy, rigid material

**Table 1** Transition temperatures (°C) and enthalpies (in parentheses, kJ $mol^{-1}$) obtained for **1[*n*]** and **2[*n*]** in the heating mode[a]

| *n* | **1[*n*]** | | | | | | | | | **2[*n*]** | | | | | | | | |
|---|---|---|---|---|---|---|---|---|---|---|---|---|---|---|---|---|---|---|
| 9 | $Cr_1$ | 99<br>(32.1) | $Cr_2$ | 140<br>(20.2) | $Cr^b$ | 154<br>(21.6) | B6 | 159<br>(17.6) | I | $Cr_1$ | 76<br>(8.2) | $Cr_2$ | 116<br>(6.4) | $Cr_3$ | 180<br>(41.9) | I | | |
| 10 | $Cr_1$ | 122<br>(27.2) | $Cr_2$ | 158<br>(47.0) | (B6 | 148)$^c$<br>(17.7) | I | | | $Cr_1$ | 82<br>(4.4) | $Cr_2$ | 94<br>(3.1) | $Cr_3$ | 107<br>(3.9) | $Cr_4$ | 180<br>(40.7) | I |
| 11 | $Cr_1$ | 118<br>(22.1) | $Cr_2$ | 157<br>(46.7) | I | | | | | $Cr_1$ | 105<br>(28.5) | $Cr_2$ | 176<br>(35.5) | I | | | | |
| 12 | $Cr_1$ | 89<br>(3.0) | $Cr_2$ | 117<br>(3.5) | $Cr_3$ | 157<br>(48.4) | I | | | $Cr_1$ | 103<br>(39.9) | $Cr_2$ | 179<br>(45.6) | I | | | | |
| 13 | $Cr_1$ | 127<br>(5.3) | $Cr_2$ | 154<br>(44.9) | I | | | | | $Cr_1$ | 108<br>(23.5) | $Cr_2$ | 176<br>(37.6) | I | | | | |

[a] Cr = crystal; B = banana phase; I = isotropic. [b] An additional Cr–Cr transition was observed at 147 °C (1.0 kJ $mol^{-1}$). [c] Monotropic transition.

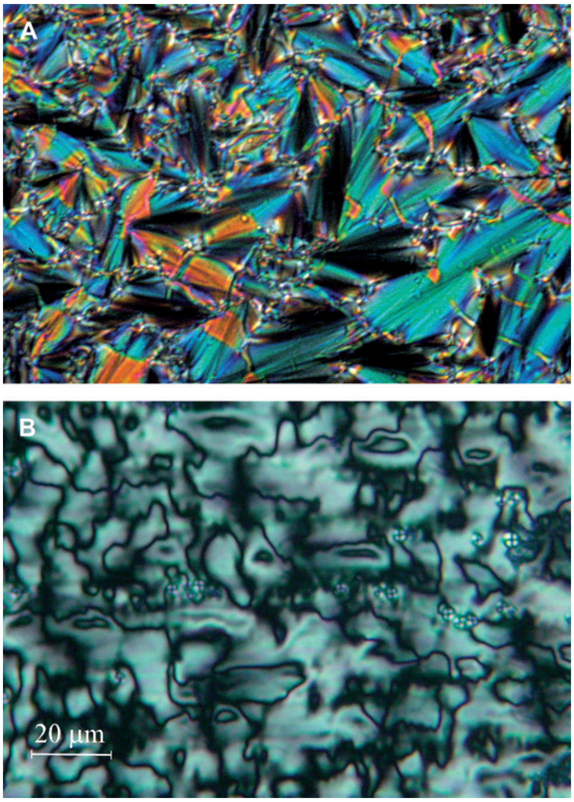

**Fig. 2** Texture photomicrographs of **1[9]** obtained on cooling to about 155 °C from the isotropic phase: (A) fan-shaped texture and (B) a schlieren texture. See text for details.

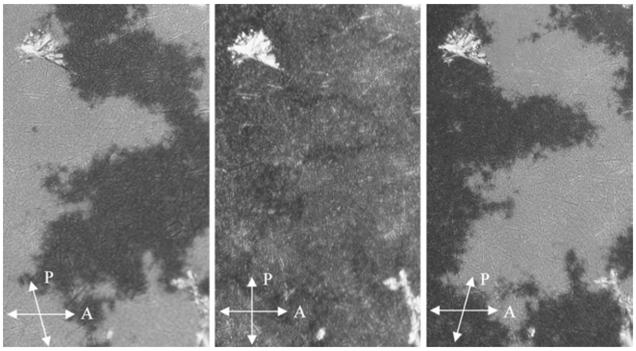

**Fig. 3** A natural texture of **2[10]** obtained upon cooling to 170 °C from the isotropic phase in the absence of electric field viewed with crossed (middle) and decrossed polarizers. Arrows indicate the polarizer configuration. A crystallite is visible in the upper-left corner.

without changing the texture. The texture observed for the monotropic phase found in **2[*n*]** could be attributed to a B4 phase.[17,18] However, this assumption could not be confirmed by XRD analysis because the metastable phase always co-exists with crystallites (Fig. 3), and easily crystallizes at temperatures near the isotropic transition.

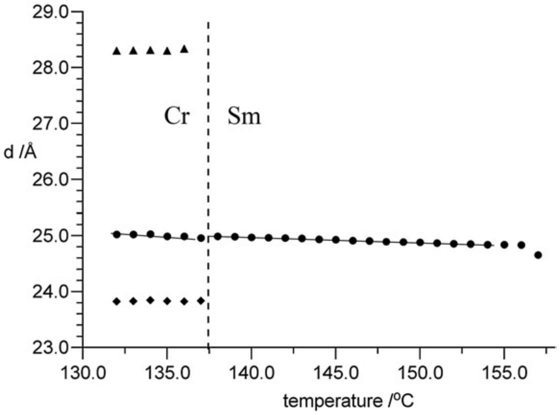

**Fig. 4** Temperature-dependent small angle reflections in the smectic and crystalline phases for **1[9]** recorded in the cooling mode. The slope is for the smectic layer spacing (circles) is $-9.5(1) \times 10^{-3}$ Å $K^{-1}$ in the range of 139–154 °C. The vertical line marks the crystallization temperature.

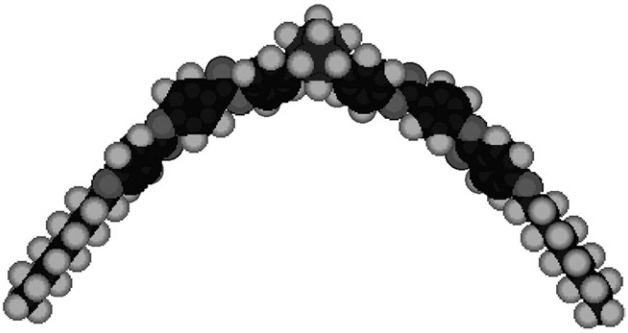

**Fig. 5** UFF optimized molecular structure of **1[9]** in the fully extended bow-like conformation. The molecule's projection on the horizontal axis is 47 Å.

## X-Ray diffraction

X-Ray powder diffraction analysis of the mesophase formed by **1[9]** revealed one reflection in the small angle region, corresponding to a smectic layer distance *d* of about 25 Å (Fig. 4). The observed layer spacing *d* is about half of the molecular length in the most extended bow-like conformation (Fig. 5), according to the calculations with the Universal Force Field (UFF) algorithm. This indicates that molecules are strongly intercalated between layers, which supports the assignment to the B6 phase ($SmA_c$).[1]

The layer spacing *d* slightly decreases with increasing temperature. This suggests increasing disorder of the nonyl chains and consequent reduction of the effective length of the alkyl substituent and contraction of the layer spacing.

Despite efforts, XRD analysis of the adamantane derivative **2[11]** showed a practically identical pattern for a virgin sample before melting and for one cooled from the isotropic phase at about 10 K below melting point (see ESI‡). This indicates that the weakly birefringent metastable phase shown in Fig. 3 either quickly crystallizes or is not formed at all under the XRD experimental conditions. It is also possible that the monotropic phase is a crystalline modification.

## Electrooptical analysis

Brief investigation of the electric field effect on the mesophase texture showed no switching behavior (no change of light

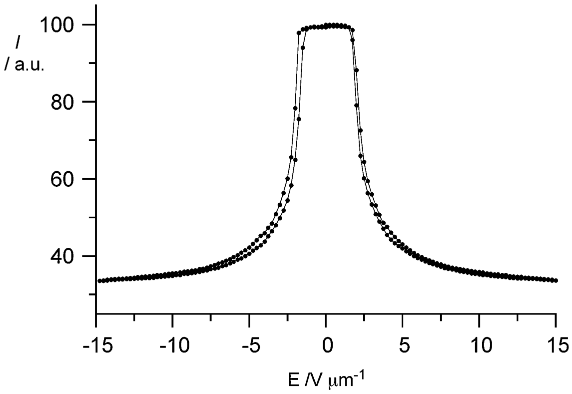

**Fig. 6** Transmission as a function of applied dc electric field obtained for a sample of **1[9]** in a standard planar 3.2 μm cell at ~155 °C.

extinction direction upon application of the field) in either series of compounds. This lack of interaction with electric field further supports the assignment of the observed mesophases as non-polar B6 for carboranes **1[*n*]** and is consistent with the possible B4[19] phase for adamantanes **2[*n*]**. It was found, however, that for **1[9]** the birefringence varies significantly and reproducibly with the applied field. The birefringence change is not accompanied by polarization switching (no current peak), and thus has a dielectric origin.

A similar effect has been observed in another bent-core mesogen,[20] and was explained by molecular rotation to orient their planes parallel to the applied field. Moreover, a well defined threshold was observed on the transmission *vs.* electric field curve (Fig. 6). The existence of the threshold, of about 2 V μm$^{-1}$ in a 3.2 μm thick cell, could be interpreted as partial breaking of molecular anchoring to the glass. Further experiments in cells with different thickness and alignment layers are necessary for a better understanding of this phenomenon.

## Discussion and conclusions

Experimental results demonstrate that compounds with a bent-core molecular architecture containing sterically demanding central groups, *m*-carborane and adamantane, form non-polar phases. Carborane derivatives **1[*n*]** exhibit an intercalated lamellar B6 phase, which is quickly destabilized with increasing length of the alkyl chain. Compounds in the adamantane series **2[*n*]** form a monotropic phase, whose optical texture and lack of interaction with electric field are consistent with a soft crystalline B4 phase. The mesophase in the carborane series appears to be destabilized relative to that in the benzene analogs. For instance, the benzene analogs of **1[9]** and **1[12]** exhibit nearly 60 K and 40 K wide, respectively, polar B1 phases (Col$_r$) with clearing temperatures of over 200 °C.[11,21] A higher homolog of the *m*-terphenyl derivative shows an antiferroelectric B2 phase (SmCP$_A$).[11]

*m*-Carborane and adamantane can be viewed as angular analogs of *p*-carborane and bicyclo[2.2.2]octane, respectively, which have been used as elements for isostructural series of rod-like liquid crystals.[22–27] Our results show that *p*-carborane derivatives typically have lower phase stability and less tendency to form lamellar phases than the carbocyclic analogs (*p*-carborane < bicyclo[2.2.2]octane, benzene). This has been ascribed, in part, to the five-fold minima for rotation around the carborane–R bond, which leads to significant conformational mobility of the substituents and overall molecular flexibility. The mobility results in difficulties in formation of lamellar phases and the compact packing arrangements in the solid phase. In contrast, both bicyclo[2.2.2]octane and adamantane analogs have three-fold rotational potentials, which results in a greater molecular rigidity. Consequently, the two carbocycles are expected to exhibit more organized phases and higher transition temperatures than the carborane analogs. This is indeed observed experimentally for both rod-like and bent-core compounds.

The present findings open new possibilities for controlling mesophase properties of bent-shaped molecules by using sterically demanding central groups. Future structural modifications in series **1[*n*]** and **2[*n*]** by desymmetrization of the substituents, partial fluorination of the alkyl groups and/or benzene rings may allow for induction of enantiotropic polar, switchable phases in *m*-carborane and adamantane derivatives. For instance, partial fluorination of the C8 tail in the analogous *m*-terphenyl series induced a broad range antiferroelectic B2 phase.[11]

## Experimental

Thermal analysis results were obtained using a TA Instruments 2920 DSC. Transition temperatures (onset) and enthalpies were obtained using small samples (1–2 mg) and a heating rate of 5 °C min$^{-1}$ under a flow of nitrogen gas. Optical microscopy and phase identification were performed using a PZO "Biolar" polarized microscope equipped with a HCS402 Instec hot stage. Electrooptical studies were carried out in 3.2 μm thick planar cells with ITO electrodes using a setup based on a Nikon Optiphot2-Pol microscope with a P102 photomultiplier. X-Ray diffraction experiments were performed with a Bruker D8 Discover system equipped with an Anton Paar DCS350 heating stage.

The preparation of intermediates and compounds in series **1[*n*]** and **2[*n*]** is described in the ESI.‡

## Acknowledgements

This work was supported in part by the NSF grant (DMR-0111657) and by a Grant-in-Aid for High Technology Research Program from the Ministry of Education, Culture, Sports, Science and Technology, Japan. XRD experiments were performed in The Structural Research Laboratory at Warsaw University, established under the European Regional Development Found Program (WKP-1/1.4.3/1/2004/72/72/165/2005) and funded in part by the ESF/2007/03 grant.

## References

1 R. A. Reddy and C. Tschierske, *J. Mater. Chem.*, 2006, **16**, 907–961.
2 M. B. Ros, J. L. Serrano, M. R. de la Fuente and C. L. Folcia, *J. Mater. Chem.*, 2005, **15**, 5093–5098.
3 G. Pelzl, S. Diele and W. Weissflog, *Adv. Mater.*, 1999, **11**, 707–724.
4 T. Niori, T. Sekine, J. Watanabe, T. Furukawa and H. Takezoe, *J. Mater. Chem.*, 1996, **6**, 1231–1233.
5 D. M. Walba, in *Topics in Stereochemistry*, ed. M. M. Green, R. J. M. Nolte and E. W. Meijer, Wiley & Sons, New York, 2003, vol. 24, pp. 475–518.
6 G. Gesekus, I. Dierking, S. Gerber, M. Wulf and V. Vill, *Liq. Cryst.*, 2004, **31**, 145–152.

7 E. Cavero, D. P. Lydon, S. Uriel, M. R. de la Fuente, J. L. Serrano and R. Giménez, *Angew. Chem., Int. Ed.*, 2007, **46**, 5175–5177.

8 R. N. Grimes, *Carboranes*, Academic Press, New York, 1970.

9 V. I. Bregadze, *Chem. Rev.*, 1992, **92**, 209–223.

10 A. W. Laubengayer and W. R. Rysz, *Inorg. Chem.*, 1965, **4**, 1513–1514.

11 D. Shen, A. Pegenau, S. Diele, I. Wirth and C. Tschierske, *J. Am. Chem. Soc.*, 2000, **122**, 1593–1601.

12 W. Wan, W.-J. Guang, K.-Q. Zhao, W.-Z. Zheng and L.-F. Zhang, *J. Organomet. Chem.*, 1998, **557**, 157–161.

13 C. Tschierske and H. Zaschke, *J. Prakt. Chem.*, 1988, **330**, 1–14.

14 R. Coult, M. A. Fox, W. R. Gill, P. L. Herbertson, J. A. H. McBride and K. Wade, *J. Organomet. Chem.*, 1993, **462**, 19–29.

15 G. Pelzl, I. Wirth and W. Weissflog, *Liq. Cryst.*, 2001, **28**, 969–972.

16 J. C. Rouillon, J. P. Marcerou, M. Laguerre, H. T. Nguyen and M. F. Achard, *J. Mater. Chem.*, 2001, **11**, 2946–2950.

17 D. M. Walba, L. Eshdat, E. Körblova and R. K. Shoemaker, *Cryst. Growth Des.*, 2005, **5**, 2091–2099.

18 F. Araoka, N. Y. Ha, Y. Kinoshita, B. Park, J. W. Wu and H. Takezoe, *Phys. Rev. Lett.*, 2005, **94**, 137801.

19 H. Niwano, M. Nakata, J. Thisayukta, D. R. Link, H. Takezoe and J. Watanabe, *J. Phys. Chem. B*, 2004, **108**, 14889–14896.

20 K. Fodor-Csorba, A. Jákli, A. Vajda, S. K. Prasad, D. S. S. Rao, R. Y. Dong, J. Xu and G. Galli, *ChemPhysChem*, 2006, **7**, 2184–2188.

21 D. Shen, S. Diele, G. Pelzl, I. Wirth and C. Tschierske, *J. Mater. Chem.*, 1999, **9**, 661–672.

22 P. Kaszynski and A. G. Douglass, *J. Organomet. Chem.*, 1999, **581**, 28–38.

23 A. Januszko, P. Kaszynski and W. Drzewinski, *J. Mater. Chem.*, 2006, **16**, 452–461.

24 A. Januszko, P. Kaszynski, M. D. Wand, K. M. More, S. Pakhomov and M. O'Neill, *J. Mater. Chem.*, 2004, **14**, 1544–1553.

25 K. Ohta, A. Januszko, P. Kaszynski, T. Nagamine, G. Sasnouski and Y. Endo, *Liq. Cryst.*, 2004, **31**, 671–682.

26 A. Januszko, K. L. Glab, P. Kaszynski, K. Patel, R. A. Lewis, G. H. Mehl and M. D. Wand, *J. Mater. Chem.*, 2006, **16**, 3183–3192.

27 B. Ringstrand, J. Vroman, D. Jensen, A. Januszko, P. Kaszynski, J. Dziaduszek and W. Drzewinski, *Liq. Cryst.*, 2005, **32**, 1061–1070.